International Journal of Aviation Science and Engineering
e-ISSN: 2715-6958 p-ISSN: 2721-5342

AVIA

Original Article

Preliminary Design of a 6-Seater Electric Aircraft

C Chandra [1,*], M Khan [1], T Putri [1], W Alexsoh[1], M A Moelyadi[1], E Amalia[1]

1 Department of Aerospace Engineering, Bandung Institute of Technology, St. Ganesha No. 10 Bandung 40132, Indonesia

* Correspondence: calvinchristianc@students.itb.ac.id; Tel.: +62-81285922547

Received: 12 August 2023; Accepted: 14 October 2023; Published: 1 December 2023

A more sustainable and eco-friendly aircraft is needed for the near future, but current electric aircraft technology (e.g., electric motors and batteries) is still lacking compared to its fossil-fuel-based counterparts. To support the effort for fully electric aircraft maturity, an electric aircraft up to its preliminary design stage is developed using various analytical and software-based analyses with the target of fulfilling a set of design requirements and objectives for a 5000 kg MTOW 6-seater fully electric aircraft. The results of the aircraft preliminary design yield that overall, the aircraft fulfills all the requirements and most of the objectives. The design itself can still be further developed through optimization, re-evaluation, future studies, and upcoming technologies.

Keywords: Aircraft Design; Electric Aircraft; Sustainability

1. Introduction

Nowadays, the means of travel using an aircraft is quite common due to the advancement of its technology. One of which is the regional transport aircraft mainly used to transport a small number of passengers or cargo over a relatively short distance [1]. This method of travel is convenient in some applications, for example, implementation in a maritime country, because of the size of the aircraft and accessibility to the target locations themselves. But it addresses one problem: the currently growing fleet of fossil-fuel-based propulsion aircraft that has a couple of future issues. One of them being the ever depleting and limited fossil fuel currently distributed around the globe. The others are the noise and air pollution associated with burning fossil fuels. One solution to these problems is the design and large-scale implementation of fully electric aircraft that use renewable energy for every aspect, including recharging. This solution is speculated to also be relatively lower in cost as some degree of renewable energy harvesters could be built in a location rather than transporting fuel to said location. However, current electric propulsion technology for conventional transport aircraft is still relatively new; therefore, it has limitations that make it less popular than fuel-based aircraft. One of those limitations is the motor technology for conventional transport aircraft itself, which is still very limited. Another is the amount of energy available onboard because current batteries still have smaller energy density than fuel. Although implementing new aircraft technologies are laborious, rigorous, and currently have limitations, the process of designing an electric aircraft is needed to help the technology's maturity (along with electric motor and battery advancement) and eventually replace the current fleet of fuel-based aircraft. To support this effort, we have developed an aircraft up to its preliminary design, including analyzing and determining aspects of the aircraft to fulfill the design requirements and objectives (DRO).

e-ISSN: 2715-6958 p-ISSN: 2721-5342

2. Materials and Methods

The design requirements and objectives (DRO) for a six-seater aircraft are obtained and used to develop e-SPaRTA. The aircraft is designed to fulfill the DRO and the regulations by using several methods already developed on several references. The DRO is tabulated in Table 1.

Table 1. e-SPaRTA's Design Requirements and Objectives

GENERAL				**PERFORMANCE**		
Capacity		6 people		Cruise Range	≥ 350 km (MTOW)	
MTOW		5000 kg	11023,11		≥ 400 km (4 passengers + 1	
CABIN AND INSTRUMENT				Cruise Altitude	3.048 km	10000 ft
Flight Deck		1 crew		Cruise Speed	240 km/h	129.6 kts
Passenger		4-5 pax		Maximum Cruise Speed	≥ 300 km/h	161.9 kts
Cabin Volume		≥ 5.5 m^3		Maximum Service Ceiling	≥ 3657.6 km	≥ 12000 ft
Luggage Capacity		≥ 0.9 m^3		Takeoff Distance	≤ 900 m	
Weight	Passenger	90 kg	198,42	Landing Distance	≤ 950 m	
Per Pax.	Luggage	10 kg	22,05 lb	Initial Rate of Climb	≥1500 fpm	
OBJECTIVE						
Price/unit		≤ 1.8 million USD		BEP	400 unit	

The aircraft may be designed using the latest technologies and consistent aerodynamics constructions, and system technologies with maximum reliability and maintainability during its lifetime.

Maximum cruising speed at 10000 ft with 0.95 maximum takeoff weight may not be less than 300 km/h

Analytical Hierarchy Process (AHP) is used to determine configuration on e-SPaRTA. AHP is a method which Thomas L. Saaty developed. This decision support model will describe the problem of complex multi-factor or multi-criteria into a hierarchy. Analytical Hierarchy Process is a method for solving a complex and unstructured situation in several components in a hierarchical arrangement by giving subjective values about each variable's relative importance and determining which variable has the highest priority to influence the outcome in that situation. The decision-making process is basically to choose the available alternatives.

Table 2. Analytical Hierarchy Process

	Weight	Alternative 1	Alternative 2	…	Alternative n
Criteria 1	W_1	A_{11}	A_{12}	…	A_{1n}
Criteria 2	W_2	A_{21}	A_{22}	…	A_{2n}
…	…	…	…	…	…
Criteria n	W_n	A_{n1}	A_{n2}	…	A_{nn}
Total	$\sum_{i=1}^{n} W_i$	$\sum_{i=1}^{n} A_{i1}W_i$	$\sum_{i=1}^{n} A_{i2}W_i$	…	$\sum_{i=1}^{n} A_{in}W_i$

The next task is to perform a constraint analysis using a special chart called a matching chart. The main advantage of this chart is that it can be used to assess the required wing area and power plant for the design, such that it will meet all requirements [2]. The matching chart of e-SPaRTA is constructed by following Roskam's method [3]. The matching chart is done by plotting the constraints on two axes, such as (y-axis) thrust-to-weight ratio (T/W) and (x-axis) wing loading (W/S). The matching chart is read by noting any combination of (W/S) and (T/W) above the constraint line, resulting in a design that meets DRO and CASR regulation.

 doi: 10.47355/AVIA.V5I2.93

e-ISSN: 2715-6958 p-ISSN: 2721-5342

The aerodynamic characteristic of an airfoil is analyzed from JavaFoil software, while the aerodynamic analysis of e-SPaRTA's full configuration is performed using United States Air Force (USAF) Stability & Control DATCOM. Results obtained from the aerodynamic analysis include coefficients of lift, drag, and moment which will be used further on stability and performance analysis of e-SPaRTA.

The weight for each aircraft's component is estimated using statistical weight estimation methods for general aviation aircraft [4]. This estimation method is based on historical data from the existing aircraft, in which it is possible to derive the relationship based on geometric parameters such as wing area, aspect ratio, taper ratio, and limit or ultimate load factor. For the aircraft's battery, the weight is estimated by calculating the product of energy required to accomplish the mission [5] with the energy density of the chosen battery. Figure 1 shows the normalized power of a typical mission profile for electric aircraft.

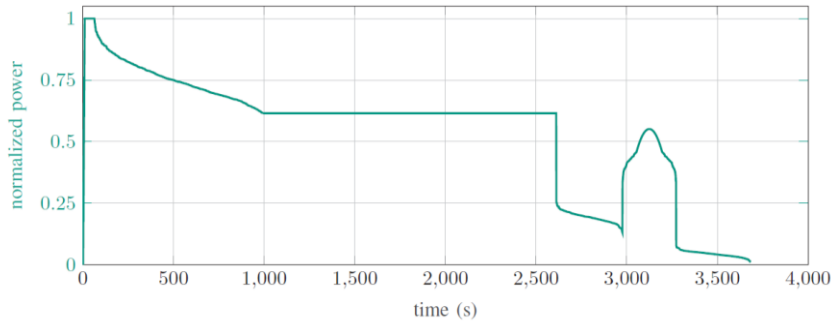

Figure 1. Normalized power of typical mission profile for hybrid-electric aircraft [5]

After calculating the weight of each aircraft's component, the next task is to estimate the location distribution for each component and calculate the center of gravity for the aircraft. The distribution for each component is estimated by following the typical location of the aircraft [6].

Stability and control include static stability and dynamic stability. In the analysis, we need to produce stable aircraft. DATCOM software is used to obtain the coefficient of aerodynamic characteristics. Then it is processed using advanced calculations using the equation in the reference [7]. Then it is compared to typical values from reference [4] to adjust the fair value for e-SPaRTA. Furthermore, the static margin and neutral point were determined using an evaluation based on the [4] reference so that the criteria that were deemed appropriate were obtained. Moreover, a simple calculation is implemented from the reference [8] to evaluate the horizontal tail control capacity. All these aspects are evaluated and iterated again to get the desired characteristics in terms of stability.

The analysis of e-SPaRTA will be divided into several categories: electric motor performance, takeoff performance, landing performance, climb performance, cruise performance, and flight envelope. The electric motor performance can be plotted using quadratic interpolation formulation [2], which represents the approximate amount of thrust produced by each motor with certain airspeed. Other performances such as takeoff and landing will be evaluated by calculating the required distance [9] and compare it to the aircraft requirement in DRO. The aircraft's maximum rate of climb is also evaluated in several flight altitudes based on the maximum available power provided by the electric motors. For the cruise performance, the aircraft's range and endurance will be evaluated using the available energy capacity from the battery and then will also be checked if it satisfies the DRO or not. On the other hand, the flight envelope of e-SPaRTA is plotted based on the CASR 23 regulation, which combines various parameters from aerodynamic, propulsion, and structure from the aircraft.

The cost of e-SPaRTA is analyzed using the preliminary design Roskam [10]. This analysis is done to assess the cost needed for the development process to manufacture process, the aircraft's price, and the profit obtained for the company. The cost analysis for e-SPaRTA accounts for multiple factors, such as the aircraft data, powerplant/ motor data, number of aircraft produced for testing, aircraft's material, the monthly rate of production, and production factor. The cost estimation is also done by considering the objective of e-SPaRTA, where the aircraft's price may not exceed 1.8 million USD.

e-ISSN: 2715-6958 p-ISSN: 2721-5342

3. Results

3.1. e-SPaRTA Configuration

The configuration result of e-SPaRTA is developed from some literature [2,8]. The configuration arrangements for e-SPaRTA are obtained considering each alternative's advantages and disadvantages. Table 3 shows the configuration that is obtained from the AHP method.

Table 3. e-SPaRTA's Aircraft Configuration

Part	Criteria	Configuration
Wing	Wing Position	High wing
	Aspect Ratio	High AR
	Planform	Trapezoidal
	Swept/ Unswept	Swept
	Dihedral Angle	Flat
	Plane	Monoplane
Fuselage	Structure	Semi-monocoque
	Geometry Shape	Tubular
Empennage	Configuration	Conventional
Landing Gear	Configuration	Tricycle
	Type	Retractable
Electric Motor	Pusher/ Puller	Puller
	Location	Wing-mounted
	Number of Motors	6 Motors

3.2. Matching Chart and Design Point

The primary purpose of creating a matching chart is to find the possible design point based on the aircraft's weight. There are two parameters in the matching chart: power loading (W/P) and wing loading (W/S). The boundaries in the matching chart are defined from the aircraft regulation, CASR 23, and existing general aircraft's aerodynamic characteristics [3]. These boundaries provide a benchmark for any design points that might not be possible for the aircraft to operate or even violate the regulation. Choosing the design point under the boundary curves will help further design in later progress. The design points chosen for e-SPaRTA are 50 N/hp of power loading and 1250 N/m² of wing loading, as shown in Figure 2.

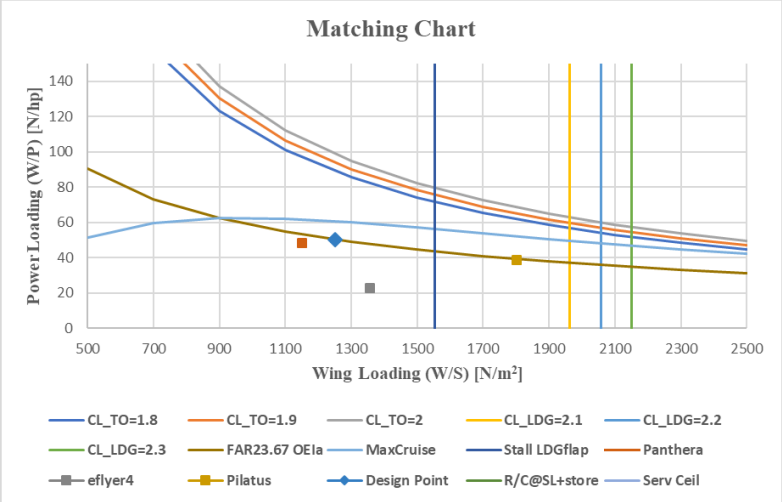

Figure 2. Matching Chart of e-SPaRTA

3.3. e-SPaRTA's Design

3.3.1. Fuselage Design

The fuselage design calculations first yield the general data for the fuselage tabulated in Table 4. All interiors are then determined, added, and arranged to the fuselage resulting in the top-, side-, and cross-section view depicted in Figure 3.

 doi: 10.47355/AVIA.V5I2.93

e-ISSN: 2715-6958 p-ISSN: 2721-5342

Table 4. General Fuselage Parameters

Parameter	Value	Unit
Fuselage Length, l_f	13.093	m
Fuselage Diameter (Height), d_f	2	m
Nose Length, l_n	3.5	m
Cabin Length, l_c	5.593	m
Tail Length, l_{fc}	4	m
Empty Cabin Volume, V_{cabin}	17.572	m^3
Tailcone Angle, θ_{fc}	21	deg

Material					
Frame & Longeron	Al 7075 -T6	Bulkhead	Steel Alloy	Skin	Al 2024-T3

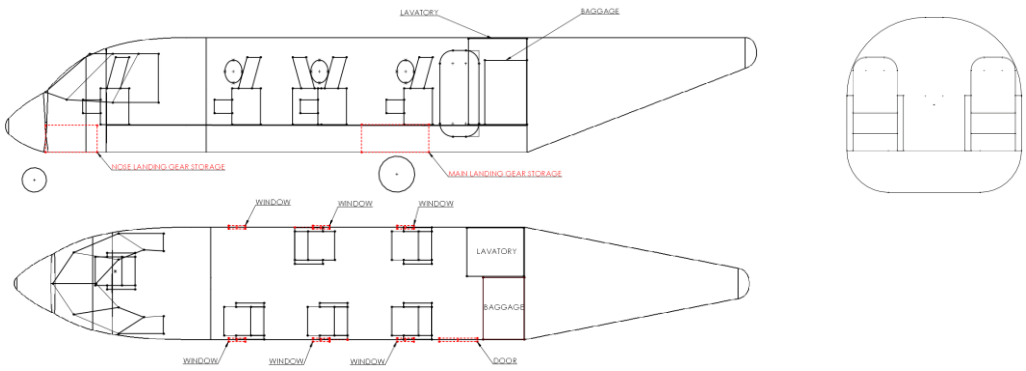

Figure 3. e-SPaRTA Fuselage Top View, Side View, and Cross-Section View

3.3.2. Wing Design

Using the wing loading from the chosen design point, the basis of the wing dimensions can be calculated. Following this, with iterations and evaluation from aerodynamic analysis, it is decided that NACA 4412 will be used as the wing's airfoil for e-SPaRTA. Other wing components such as ailerons and flaps are designed based on the structural considerations, motor position, and the general position from existing aircraft [4].

Table 5. e-SPaRTA's Wing Geometry Data

Wing Dimension		Aileron Sizing		Flap Sizing	
Wing loading (N/m^2)	1250	Position (m)	5.97-9.45	Position (m)	1.26-5.87
Wing Area (m^2)	39.24	Span (m)	3.48	Span (m)	4.61
Wing Span (m)	20.30	Chord (%)	25.0	Chord (%)	25
Taper ratio	0.40				
Root Chord (m)	2.76	**Airfoil Data (NACA 4412)**			
Tip Chord (m)	1.10	Maximum Thickness (% chord)		12	
MAC (m)	2.05	Thickness Location (% chord)		30	
Swept Angle (°)	0.00	Camber (% chord)		4	
Dihedral Angle (°)	0.00	Camber location (% chord)		40	

Material			
Spar, Ribs, Stringer	Al 7075	Skin Panel	Al 2024

 doi: 10.47355/AVIA.V5I2.93

e-ISSN: 2715-6958 p-ISSN: 2721-5342

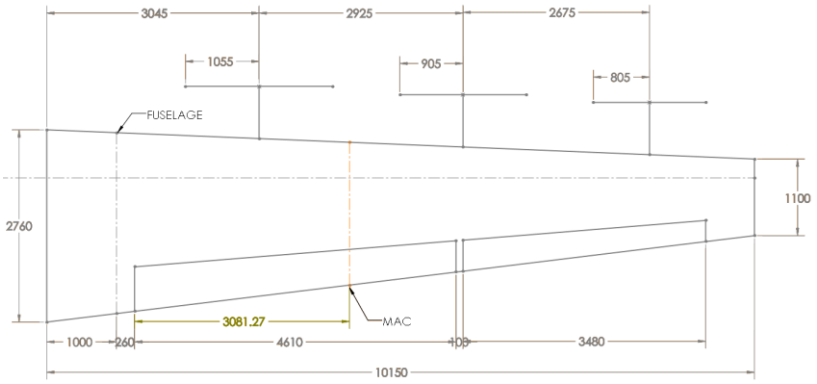

Figure 4. e-SPaRTA's Wing Design

3.3.3. Empennage Design

The empennage sizing adapted from the general aviation manual handbook to get the initial sizing for vertical and horizontal tail refers to reference [2]. Sizing of control surfaces refers to reference [4] with an adjustment and structure consideration. The chosen airfoil for the empennage design is NACA 0012.

Table 6. Empennage Sizing

Empennage Dimension			**Control Surfaces**			
Variable	**VTP**	**HTP**	**Elevator**		**Rudder**	
Chord	2.53	2.00	Position (m)	0.442-2.95	Position (m)	0.262-2.955
Area (m²)	3.84	5.55	Span (m)	2.95	Span (m)	3.28
Span (m)	8.30	11.99	Chord (%)	36	Chord (%)	30
Taper ratio	3.28	6.00				
Root Chord (m)	0.60	0.50	**Airfoil Data (NACA 0012)**			
Tip Chord (m)	2.70	2.67	Maximum Thickness (% chord)		12	
MAC (m)	1.62	1.33	Thickness Location (%) chord)		30	
Swept Angle (°)	2.20	2.07	Camber (% chord)		0	
Dihedral Angle (°)	20.00	5.00	Camber location (% chord)		0	

Material			
Ribs, Spar, & Stringer	Al-7075	Skin panel	Al- 2024

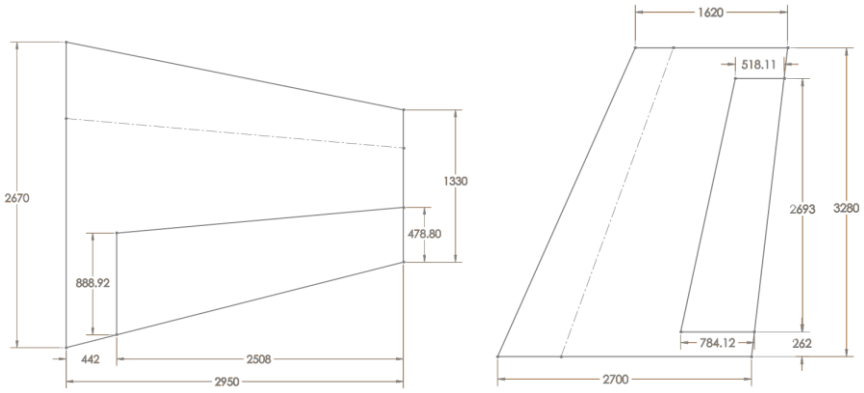

(a) (b)

Figure 5. e-SPaRTA's (a) Horizontal Tailplane; (b) Vertical Tailplane Design

 doi: 10.47355/AVIA.V5I2.93

e-ISSN: 2715-6958 p-ISSN: 2721-5342

3.3.4. Electric Motor Selection

Using the power loading from the chosen design point, the power needed from the motors can be estimated, which is about 731.54 kW. The decided design will use six electric motors because more motors will provide more safety in case of motor failure. Furthermore, it will distribute the wing load more evenly and give less drag to the aircraft.

There will be three pairs of electric motors selected from EMRAX electric engine manufacturer: EMRAX 268, EMRAX 228, and EMRAX 208. They are positioned with EMRAX 268 closest to the wing root, while EMRAX 208 is placed nearest to the wingtip. The propeller for each motor is designed with two blades and the diameter is estimated based on the power needed to be produced from each motor [4].

Table 7. Electric Motor Data

EMRAX Series	Peak Power (kW)	Continuous Power (kW)	Length (mm)	Diameter (mm)	Mass (kg)	Max. Battery Voltage (Vdc)	Max. RPM	Efficiency (%)	Propeller Diameter (m)
268	200	107	91	268	20.3	250	4500	92-98	2.11
228	109	62	86	228	12.3	160	5500	92-98	1.81
208	68	41	85	208	9.3	120	6000	92-98	1.61

3.3.5. Battery Selection

The battery selection is done by considering the required energy to accomplish the mission and the energy density of the battery. The battery's energy density describes how much power the battery can produce in an hour for every kilogram of battery; thus, the higher energy density will result in lighter battery weight. By researching the available aircraft battery on the market, a suitable battery for e-SPaRTA is found with specifications as shown in Table 8.

Table 8. Selected Battery for e-SPaRTA

Manufacturer	Battery Type	Energy Density (Wh/kg)	Efficiency (%)
Sion Power (Licerion HE)	Li-S	490	99.70

3.4. Aerodynamic Analysis

The aerodynamic analysis is performed using DATCOM. There are 3 flight conditions that will be evaluated: clean (cruise), takeoff, and landing. Firstly, one crucial parameter that needs to be considered in aircraft aerodynamics is the lift. Since the lift required by an aircraft for takeoff and landing is typically higher than on cruise, most aircraft are equipped with high lift devices. High lift devices used in e-SPaRTA are single-slotted flaps designed to be operated at 5° for takeoff and 20° for landing. These configurations will provide a higher lift for the e-SPaRTA, as shown in Figure 6(a).

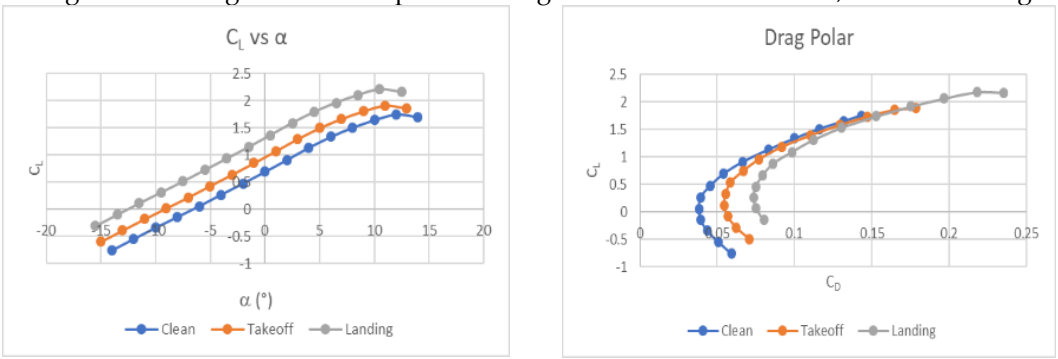

(a) (b)

Figure 6. e-SPaRTA's (a) Lift Coefficent; (b) Polar Drag

Another important parameter that must be considered is drag. Note that using high lift devices not only will increase the lift but also the amount of drag. This phenomenon can be seen by plotting

e-ISSN: 2715-6958 p-ISSN: 2721-5342

the drag polar curve. Following this, the aircraft's aerodynamic efficiency can be evaluated by comparing the lift to drag ratio in cruise conditions with the maximum possible value of lift to drag. The closer the value means, the more efficient the aircraft is since the cruise is supposedly the longest phase in an aircraft's flight phase. e-SPaRTA has an aerodynamic efficiency of 88.23%.

3.5. Weight and Balance Analysis

Below are the general weight breakdown for e-SPaRTA and its percentage to the MTOW. The battery weight to power up the motor is calculated by considering the energy required to accomplish the mission and the battery's energy of density.

Table 9. General e-SPaRTA Weight Breakdown

Component Group	Weight	(%MTOW)
Structure (incl. motor)	1472.46	29.55
Fixed Equipment	607.76	12.19
Battery (for propulsion)	1963.02	39.41
Battery (for interior)	250	5.01
Crew & Payload	690	13.84
TOTAL	4980.24	100

The center of gravity for e-SPaRTA is analyzed for three various configurations: the design CG, most forward CG, and most aft CG. The CG range of e-SPaRTA is shown in Table 10.

Table 10. Center of Gravity Range of e-SPaRTA

Configuration	X_{ca} (m)	Z_{ca} (m)
Design	6.065	
Most Forward CG	5.935	1.57
Most Aft CG	6.123	

3.6. Structural Layout

3.6.1. Wing Structural Layout

The wing's structure consists of 2 spars, 12 stringers, and 14 ribs. These components' initial position is determined based on the critical position where structure ought to be present, motor positions, for instance. Then the rest of the wing components will be positioned using typical spacing used in existing aircraft and the consideration of aileron and flap position.

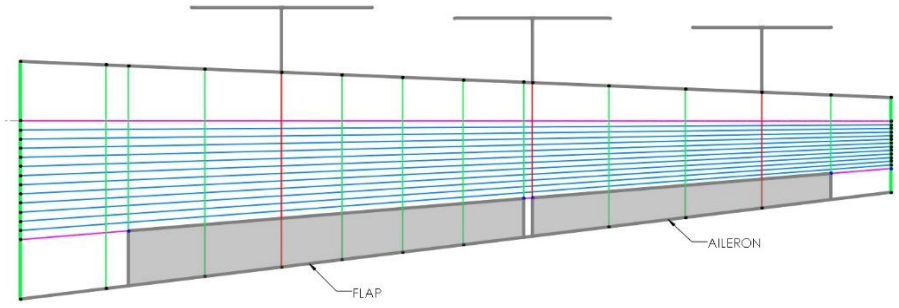

Figure 7. e-SPaRTA's Wing Structural Layout

e-ISSN: 2715-6958 p-ISSN: 2721-5342

3.6.2. Empennage Structural Layout

e-SPaRTA uses an integrated skin-stringer configuration which applies Z-stringer as stringer configuration. The configuration is determined by consideration of critical position depending on the location of the elevator and rudder. The rest of the spacing configuration uses typical spacing, referring to reference [11]. The empennage structure layout is shown in Figure 8.

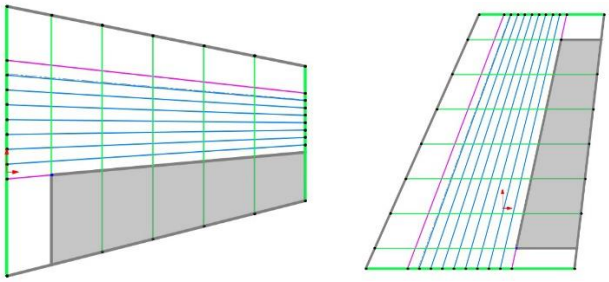

(a) (b)

Figure 8. e-SPaRTA's (a) Horizontal Tail; (b) Vertical Tail Structural Layout

3.6.3. Fuselage Structural Layout

The fuselage structural layout is determined by first placing the bulkheads and crucial longerons to withstand the high loadings on the fuselage. The remaining frames and longeron are then inserted to reinforce the fuselage structure further. The resulting layout is depicted in Figure 9, with red lines depicting bulkheads, green lines depicting frames, and blue and magenta lines (or circles) depicting the longerons.

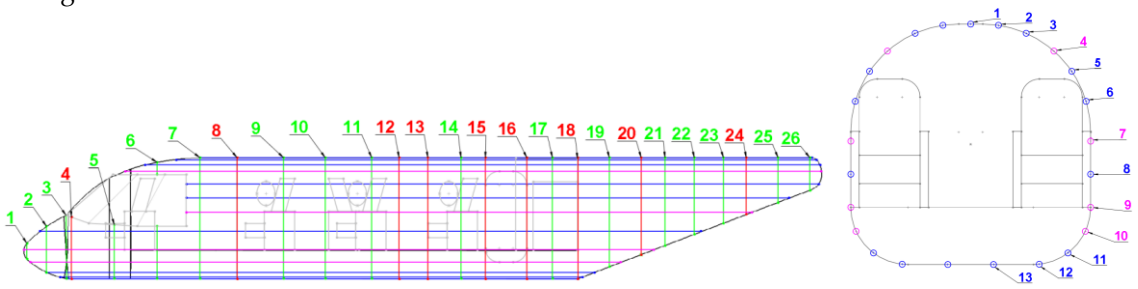

Figure 9. e-SPaRTA Fuselage Structural Layout

3.7. Landing Gear Design

3.7.1. Longitudinal Criteria Fulfillment

The fulfillment of longitudinal criteria is related to the longitudinal tip-over angle and tipback angle [4,12]. The Criteria and results (using MS Excel solver) are tabulated in Table 11. These two criteria are used to determine the overall height of the landing gear, $h_{landing\ gear}$ which is obtained to be 690 mm.

Table 11. Landing Gear Height Calculation and Longitudinal Criteria Fulfillment

Longitudinal Tip-Over			**Criteria Requirement**
Tip-Over Angle	17.03	deg	Larger than 15° or tipback angle, whichever is larger
Ground Clearance			**Criteria Requirement**
Tipback Angle	16.91	deg	Larger than 15°
Landing Gear Height			
angle diff	0.12	deg	
h_{LG}	690	mm	

 doi: 10.47355/AVIA.V5I2.93

e-ISSN: 2715-6958 p-ISSN: 2721-5342

3.7.2. Lateral Criteria Fulfillment

The lateral tip-over criteria [12] is used to obtain the lateral distance between the main landing gears, d_{MLG} which is obtained to be 3935 mm. The values of d_{MLG} and $h_{landing\ gear}$ are then used to check the lateral ground clearance criteria [12] states the space in a 5° angle measured from the surface inwards to the aircraft must be free of any components. Using SOLIDWORKS, an accurate simplified representation of the aircraft is drawn and confirmed that it fulfills the criteria.

3.7.3. Turnover Criteria Fulfillment

The turnover criteria [4] is obtained using SOLIDWORKS. Using the current aircraft configuration, it is obtained that the turnover angle is 57.36° which fulfills the criteria requirement of the turnover angle being less than 63°.

3.7.4. Maximum Load on Each Strut

The maximum load on each strut is calculated using structure statics [4,12] with the addition of dynamic nose gear load formula [4]. The analysis is done for 3 CG conditions: most forward, design MTOW, and most aft. The calculations are all done using MS Excel, with the results tabulated in Table 12.

Table 12. Maximum Load on Each Landing Gear Strut

Parameter	Total value (N)	Number of strut(s)	Load on each strut (N)	Load on each strut (lbf)
Maximum total static MLG load	42994.91	2	21497.45538	4832.82
Maximum total static NLG load	6410.69	1	6410.69	1441.18
Maximum total NLG load	8774.58	1	8774.58	1972.6

3.7.5. Tire Sizing

The tires are also a crucial part of the landing gear; it supports the aircraft at the ground and helps absorb the aircraft's kinetic energy during impact with the ground. The important design parameters of the tire are pressure, width, diameter, contact area, and rolling radius [4].

Table 13. Landing Gear Tire Sizing Data

	Main Landing Gear (MLG)	Nose Landing Gear (NLG)
Load on Tire (kN)	21.497	6.411
Pressure (kPa)	482.633	289.580
Tire Contact Area (m^2)	0.0445	0.0221
Diameter (m)	0.627	0.427
Width (m)	0.208	0.150
Rolling Radius (m)	0.260	0.175

3.7.6. Shock Absorber

Other essential components in landing gear are shock absorbers. The primary purpose of the shock absorbers is to absorb an aircraft's kinetic energy during landing impact. In e-SPaRTA, oleo shock-strut is used as the shock absorber since oleo is commonly used in many aircraft and has relatively high shock-absorbing efficiency (65-90%) [4]. The key parameter from the shock-absorbing mechanism is the deflection distance from the shock absorber called stroke. The longer the stroke, the more energy it can absorb.

Table 14. Shock Absorber Design Data

	Main Landing Gear (MLG)	Nose Landing Gear (NLG)
Kinetic Energy (kJ)	100.683	3.002
Gear Load Factor	3	3
Load on Landing Gear (kN)	64.492	19.232

e-ISSN: 2715-6958 p-ISSN: 2721-5342

Tire		
Shock-Absorbing Efficiency	0.47	0.47
Stroke (m)	0.054	0.038
Shock Absorber		
Shock-Absorbing Efficiency	0.75	0.75
Stroke (m)	0.175	0.184
Stroke with Safety Margin	0.205	0.214

3.7.7. Landing Gear Retraction System

All of e-SPaRTA's landing gear is retracted directly into the fuselage subfloor. The nose landing gear is retracted using a variation of the four-bar linkage, which is retracted towards the aircraft's aft, shown in Figure 10 (a). Meanwhile, the main landing gear is retracted using a combination of folded linkages and a hydraulic system, as shown in Figure 10 (b).

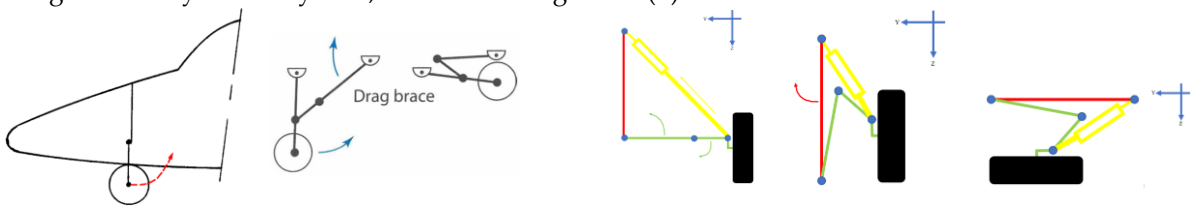

(a) (b)

Figure 10. (a) Nose Landing Gear; (b) Main Landing Gear Retraction System

3.8. Stability Analysis

The stability iteration derives some aerodynamic characteristic coefficients, tabulated in Table 15. If the results are not enough to fulfill stability requirements, they must be reevaluated. The final result represents stability data from the last configuration. There are three parameters for longitudinal static stability and six for lateral-directional stability

Table 15. e-SPaRTA's Longitudinal and Lateral-Directional Static Stability

Longitudinal Static Stability						**Lateral-Directional Static Stability**					
Derivatives	**Most Forward**		**Most Aft CG**		**Requirement**	**Derivatives**	**Most Forward**		**Most Aft CG**		**Requirement**
	/deg	**/rad**	**/deg**	**/rad**			**/deg**	**/rad**	**/deg**	**/rad**	
$C_{m\alpha}$	-0.015	-0.86	-	-	<0	$C_{Y\beta}$	-0.0018	-0.11	-0.0018	-0.11	<0
C_{mq}	-0.02	-1.15	-0.018	-	<0	$C_{n\beta}$	0.00032	0.019	0.00025	0.014	>0
$C_{L\alpha}$	0.1	5.75	0.1	5.75	>0	$C_{l\beta}$	-0.00009	-0.0052	-	-	<0
						C_{lp}	-0.00023	-0.013	-	-0.013	<0
						C_{nr}	-0.11	-6.3	-0.1	-5.8	<0

Control capacity of the horizontal tail is evaluated from some method in reference [8]. The calculation produces several values to consider for the horizontal tail design. Two parameters determine the design point of e-SPaRTA for horizontal tail configuration. The first one is the ratio of HTP-wing area, and another one is the location of CG. The result can be visualized in Figure 11.

e-ISSN: 2715-6958 p-ISSN: 2721-5342

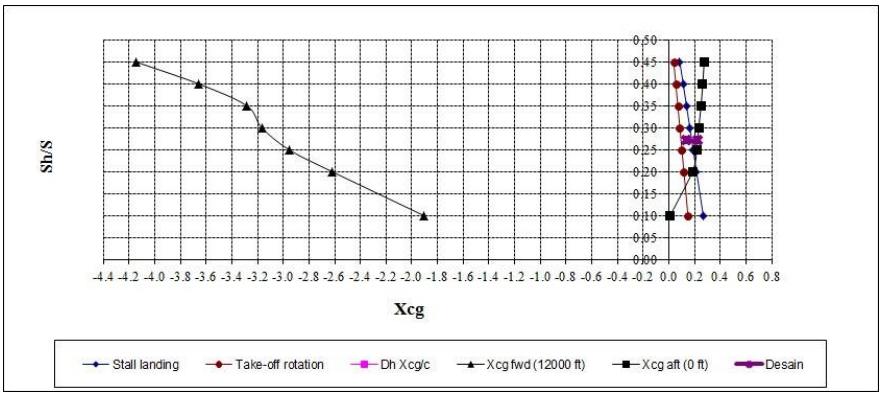

Figure 11. e-SPaRTA's HTP Design Point

3.9. Performance Analysis

3.9.1. Electric Motor Performance

For each motor in e-SPaRTA, the electric motor performance is plotted using quadratic interpolation formulation [2] in several altitude varieties.

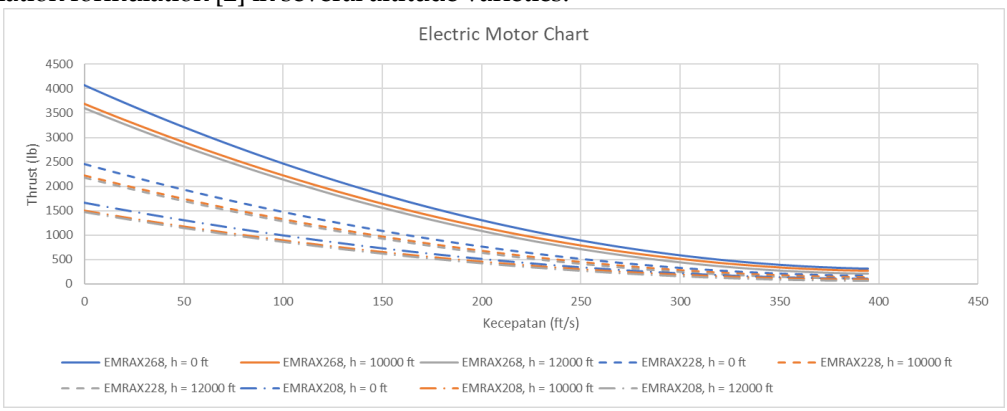

Figure 12. Electric Motor Chart

3.9.2. Takeoff Performance

In general, takeoff performance consists of two types of distance: ground distance (S_g) and airborne distance (S_a) [9]. Summing both of these distances will result in the required distance for the aircraft to takeoff (S_{TO}). But also note that the takeoff distance will also need to be multiplied by a factor of 1.15 [13].

Table 16. e-SPaRTA's Required Takeoff Distance at MTOW

Mass (kg)	T (N)	T/W	V_{stall} (m/s)	V_{LOF} (m/s)	W/S (N/m^2)	S_g (m)	R (m)	γ_c	S_a (m)	S_{TO} (m)
4980.24	32659.14	0.67	33.45	40.14	1245.06	133.55	1095.12	9.57	182.06	362.96

Another important consideration in designing multi-motor aircraft is the case of motor failure. When there is one motor or engine failure that occurs, the pilot will have to decide whether to abort or continue the takeoff. However, there is a distance limit where the aircraft is still allowed to abort the takeoff. This limit is called balance field length (BFL), and the critical velocity at this distance is called decision speed (V1).

Table 17. e-SPaRTA's BFL and V1 at Various Failure Cases

	1 EMRAX 268 Failure	1 EMRAX 228 Failure	1 EMRAX 208 Failure
BFL (m)	330.69	323.66	320.74
V1 (m/s)	33.81	33.58	33.48

 doi: 10.47355/AVIA.V5I2.93

e-ISSN: 2715-6958 p-ISSN: 2721-5342

3.9.3. Landing Performance

Similar to the takeoff performance, there are generally two types of distance: airborne distance (S_a) and ground distance (S_g) [9]. The ground distance can be divided further into the rotation phase and braking phase. Summing all these distances will result in the required landing distance of the aircraft.

Table 18. e-SPaRTA's Required Landing Distance

S_a	Rotation Distance (S_{g1})	Braking Distance (S_{g2})	S_g	Landing Distance (S_{LDG})
305.08 m	472.09 m	24.19 m	496.28 m	801.36 m

3.9.4. Climb Performance

The calculation of the climb performance will refer to its maximum rate of climb (RoC) with all the electric motors operational, which is a function of available energy, required energy, and aircraft weight. To obtain the maximum RoC, then the required energy is minimalized. The results are calculated using MS Excel and are tabulated in Table 19.

Table 19. Maximum Rate of Climb with All Electric Motors Operational

Altitude (ft)	Max Available Power, $P_{a,max}$ (Watt)	ρ (kg/m³)	Max RoC (m/s)	Max RoC (fpm)
0	640900	1.225	10.668	2099.9897
10000	527800	0.9046	7.952	1565.3475
12000	414700	0.8491	5.5453	1091.5953

3.9.5. Service Ceiling

The service ceiling is defined as the altitude at which the rate of climb has a value of 0.5 m/s. It is calculated from an equation obtained from doing a linear regression on the curve of altitude to rate of climb (m/s) with the data from Table 19. Result of the calculation yield the service ceiling of e-SPaRTA with all the electric motors operational is 25247.45 ft.

3.9.6. Cruise Performance

In cruise performance, the aircraft's range and endurance are the most common parameter to be evaluated. By knowing the amount of battery allocated for the cruise, the range and endurance can be calculated using the available amount of energy provided by the battery.

Table 20. e-SPaRTA's Cruise Performance

	MTOW	4 Pax
Battery Mass for Cruise (kg)	1106.41	
Battery Energy Density (Wh/kg)	490	
Battery Energy (MJ)	1951.71	
L/D (@10000 ft, 240 km/h)	12.77	
Maximum Cruise Speed (km/h)	316.3	
W (N)	48856.16	47973.26
Range (km)	510.11	519.50
Endurance (hour)	2.13	2.16

3.9.7. Flight Envelope

The flight envelope is a combination of maneuver and gust V-n diagram used to determine the safe operating structural load factor limit as a function of airspeed. It is calculated with the method from "Aircraft Performance Analysis" [14] and referencing [13] for some of the parameters. The maneuver V-n utilize the aircraft at MTOW, meanwhile implementing operational empty weight for the gust V-n diagram. Then, The obtained flight envelope is depicted in Figure 13.

e-ISSN: 2715-6958 p-ISSN: 2721-5342

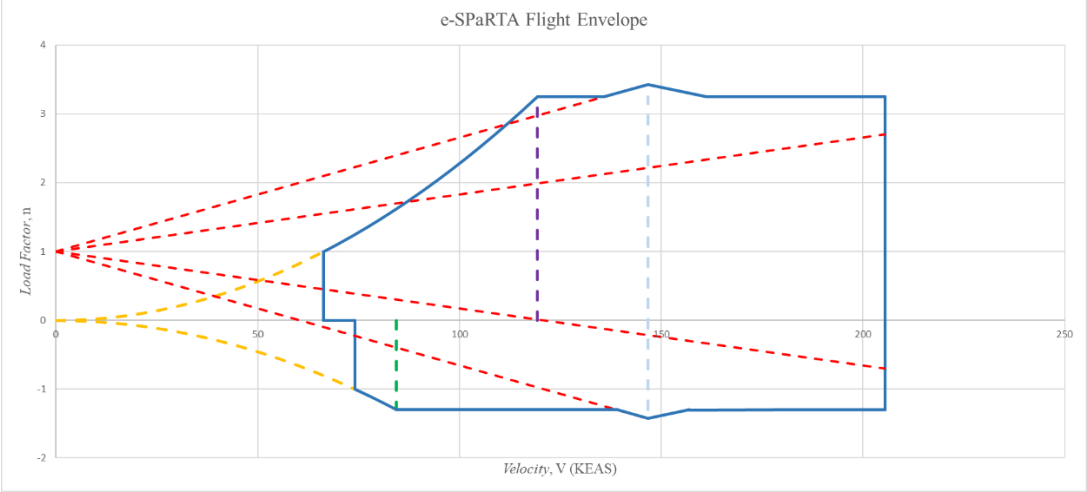

Figure 13. e-SPaRTA's Flight Envelope

3.10. Cost Analysis

The estimated purchase price for e-SPaRTA is obtained by averaging the calculated purchase price for three different methods: Roskam's method [10], Raymer's method [4], and Nicholai's method. Figure 14 shows the estimated purchase price for e-SPaRTA in design and base year for each method. As can be seen, the purchase price of the aircraft for three different methods will decrease as the production quantity increase.

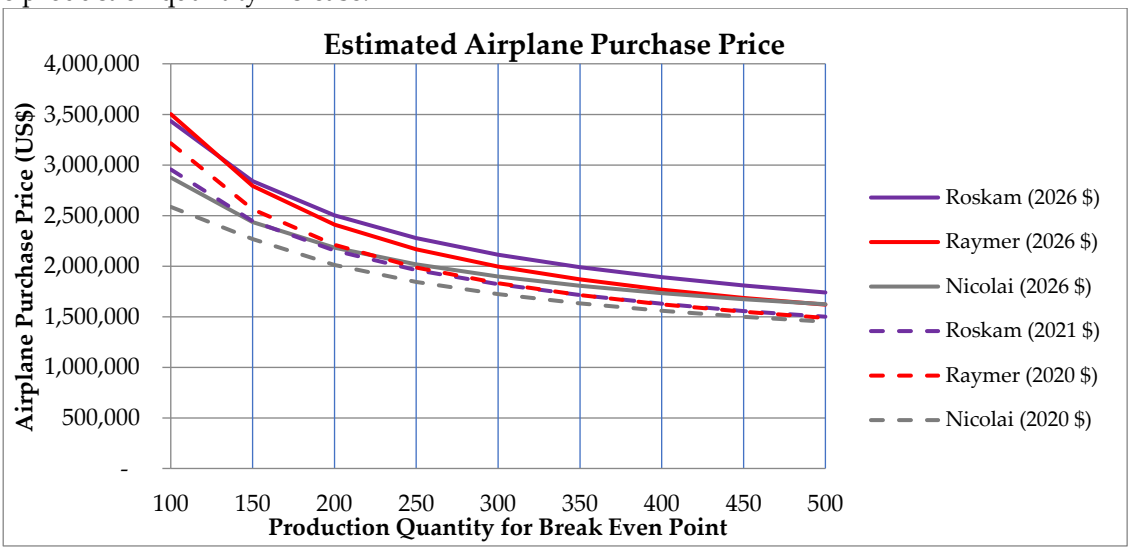

Figure 14. Estimated Purchase Price vs. Production Quantity

Table 21. Estimated Purchase Price for e-SPaRTA

Production Quantity : 400	**2021**	**2026**
Roskam (USD)	1,627,223	1,889,760
Raymer (USD)	1,622,239	1,767,338
Nicholai (USD)	1,559,134	1,733,914
Average Purchase Price (USD)		**1,797,003.97**

Using the number of BEP in DRO, 400 units, the estimated purchase price for e-SPaRTA in the design year (2026) satisfies the objective price.

e-ISSN: 2715-6958 p-ISSN: 2721-5342

4. Discussion

Referring to the results, comparing it to the DRO, it is evident that the current configuration of e-SPaRTA fulfills all of the design requirements and objectives; some even exceed it. But as it stands, e-SPaRTA's quality on every aspect can be balanced to achieve a better overall aircraft quality. This can be done by reviewing the current configuration and performing optimization on several key aspects, then redoing the analyses from the point of change, for instance: optimizing weight & balance and reevaluating stability analysis of the aircraft. Another form of optimization that can be done is by introducing new and more advanced technology (e.g., electric motor or battery) that will increase the capability of e-SPaRTA.

5. Conclusions

The preliminary design of the 6-seater electric aircraft, e-SPaRTA, shows the capability to fulfill all the desired performance and requirements in the requested DRO. However, the result of this design can still be developed further through optimization and re-evaluation followed by future studies and upcoming technologies.

References

1. E. A. E. Rodas, J. Lewe, D. N. Mavris, Feasibility Focused Design of Electric On-demands Aircraft Concepts, 2014.
2. S. Gudmundsson, General Aviation Aircraft Design: Applied Methods and Procedures, 1st ed.; ELSEVIER: Oxford, UK, 2014.
3. J. Roskam, Part I: Preliminary Sizing of Airplanes, DARcorporation: Kansas, USA, 1990.
4. D.P Raymer, Aircraft Design: A Conceptual Approach, 6th ed.; AAIA: Blacksburg, Virginia, 2018.
5. Jux B, Foitzik S, and Doppelbauer M 2018 A Standard Mission Profile for Hybrid-Electric Regional Aircraft based on Web Flight Data (Karlsruhe: Inst. Of Electrical Engineering).
6. M. H. Sadraey, Aircraft Design: A System Engineering Approach, 1st ed.; John Wiley & Sons Ltd: West Sussex, UK, 2013.
7. Prof. Dr. Hari Muhammad, Dr. Yazdi I Jenie l, AE3220 Flight Dynamics, Faculty of Mechanical and Aerospace Engineering ITB: Bandung, 2021.
8. E. Torenbeek, Synthesis of Subsonic Airplane Design; Delft University Press: Delft, Netherlands, 1982.
9. Ruijgrok G.J.J, Elements of Airplane Performance, 2nd ed.; VSSD: Delft, Netherlands, 2009.
10. .J. Roskam, Part VIII: Airplane Cost Estimation: Design, Development, Manufacturing and Operating, DARcorporation: Kansas, USA, 1990.
11. J. Roskam, Part III: Layout Design of Cockpit, Fuselage, Wing, and Empennage: Cutaways and Inboard Profiles, Kansas: Design, Analysis, and Research Corporation, 2002.
12. J. Roskam, Part II: Preliminary Configuration Design and Integration of the Propulsion System, Lawrence: DARcorporation, 1997.
13. CASR 23.. Airworthiness Standards: Normal, Utility, Acrobatic, and Commuter Category Airplanes. Indonesia: Ministry of Transportation.
14. M Sadraey, Aircraft Performance: Analysis; VDM Verlag Dr. Müller: Saarbrücken, Germany, 2011.